Optical system alignment via optical state estimation using wavefront measurements

Norbert Sigrist, David C. Redding, John Z. Lou, Yan Zhang, Scott Basinger

Jet Propulsion Laboratory, California Institute of Technology, Pasadena CA 91109, U.S.A.

ABSTRACT

Optical State Estimation provides a framework for both separating errors in test optics from the target system and deducing the state of multiple optics in a telescope beam train using wavefront as well as pre-test component measurements including the knowledge of their level of error.[1] Using this framework, we investigate the feasibility of simplifying the interferometric alignment configuration of NASA's James Webb Space Telescope, a large segmented-aperture cryogenic telescope, using a single, static auto-collimating flat instead of six such flats, resulting in a reduced sub-aperture sampling.

Keywords: optical testing, segmented mirror, space telescope, state estimation

1. INTRODUCTION

The introduction of test-specific optics will often be necessary when testing optical systems. These additional optical components are not perfect, e.g., errors in alignment, figure, surface properties, etc., and will therefore contribute to the overall errors. Unlike other optical systems where the errors may be calibrated out, large optical systems are more challenging in the sense that the test configuration add errors that are difficult to separate, cannot mimic the operational environment of the optical system completely or adequately, add errors that are test specific only, etc. Light-weight, cryogenic space telescopes such as the James Webb Space Telescope (JWST) are more challenging where the test may be conducted in a significantly different environment and where calibration of the test optics is too costly or even impossible.

The focus of this paper is to present our quick investigation of the feasibility of aligning a large telescope-type optical system with a reduced set of test-specific optical elements. This quick feasibility study is based upon the the work of Redding at al.,[1] where it was shown that Optical State Estimation (OSE) provides a framework for both separating errors in the test optics from the target system and deducing the state of multiple optics in an optical train such as that present in the JWST, which shall also be the target system of this feasibility study. In many cases, it is applicable to use the OSE to re-align the optical system close to its prescription state and then use wavefront error (WFE) minimisation algorithms to align the system for best optical performance. However, it some events, the OSE by itself is preferable since a WFE minimisation approach will do as requested but when removing the test optics, the optical system by itself performs very poorly. In this case, the test optics permitted to conceal the actual state of misalignment of the optical system.

JWST is NASA's next-generation space telescope and is also a key element of NASA's Origins Program.[2] It will have sufficient sensitivities, resolution and fields to perform a deep-field observation faster and deeper than Hubble. JWST is a six meter, 18-segmented-aperture, cryogenic, space telescope for visible and infrared astronomy. It is an actively controlled telescope in the sense that all of the primary mirror segments defining the primary mirror, the secondary mirror and the fine-steering mirror can be actuated and can therefore be adjusted to correct the optical state of the telescope in order to correct deployment errors after launch and to adjust periodically its optical state, i.e., wavefront maintenance, to correct for structural deformations, for instance.

2. MODELLING JWST'S TESTING CONFIGURATION

JWST will be integrated and tested in the large cryogenic vacuum chamber at Johnson Space Centre (JSC) in Houston, Texas. The JSC chamber will be upgraded for the testing and naturally also equipped with He and N_2 shrouds that should permit operation of the JWST at approximately orbital temperature; though, the testing is performed without the effect of having the sun-shield in place. In a possible testing configuration, JWST

Optical Fabrication, Testing, and Metrology II, edited by Angela Duparré, Roland Geyl, Lingli Wang,
Proceedings of SPIE Vol. 5965 (SPIE, Bellingham, WA, 2005) · 0277-786X/05/$15 · doi: 10.1117/12.630886

will probably be tested with the telescope facing up. Sensitive elements will be supported by gravity off-loading mechanism that are not designed to work in gravity environments like latches and hinges. Gravity sag influences cannot be eliminated and will be a significant deviation from orbital conditions. The mirrors have been polished for the zero gravity environment and departure from this "nominal" figure shape can be significant.

In this feasibility study, we assume, for simplicity, the alignment of JWST's Optical Element Telescope (OTE) only, i.e., prior to the installation of the various science instruments. The OTE, our target system, consists of 18 Primary Mirror Segment Elements (PMSE), defining the Primary Mirror (PM), a Secondary Mirror (SM), a Tertiary Mirror (TM) and a Fine-Steering Mirror (FSM). Basically, it is an all-reflective, quasi on-axis, three-mirror anastigmat (TMA) form, with the addition of a FSM near the exit pupil. As with most on-axis TMA systems, it is used off-axis in field to enable beam clearance after the tertiary mirror. The focal surface is curved, with its radius matched to the FSM to focal surface distance, which ensures no defocus effects with FSM operation. The PM and SM share a common optical axis, while the TM and FSM are decentered, but not tilted, with respect to this axis. The focal surface is both decentered and tilted from this axis. The PM, SM and TM have conic contours (ellipse, hyperbola, ellipse), while the FSM is a flat.

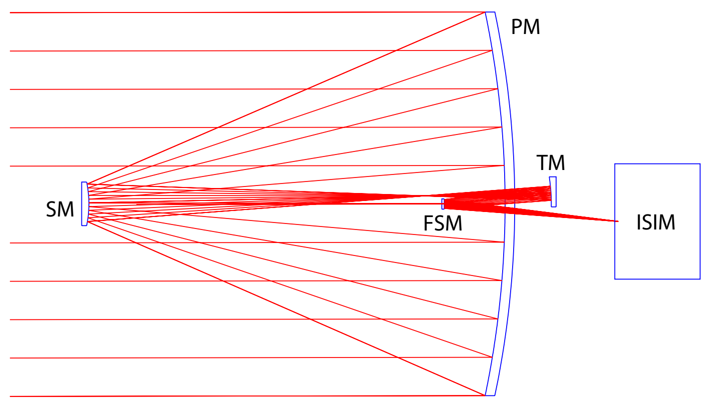

Fig. 1: On-Orbit configuration of JWST's OTE with the Integrated Science Instrument Module (ISIM) with centre of field of view associated ray fan.

OTE's PM is tested via null-lens configuration (see Fig. 2(c)) while the entire OTE is tested in a double-pass configuration in form of a sampled-aperture test (see Fig. 2(a)). Both tests requiring additional test optics consisting of null-lens specific optics in the former case and a single monolithic auto-collimating flat (ACF) in the later case. We assume that for the metrology systems we have two multi-wavelength interferometers (MWLI) to our disposition, where one is located near the Centre-of-Curvature (CoC) of the PM observing the PM via null optics only and defines the CoC metrology system while the other is located in the Integrated Science Instrument Module (ISIM) at the OTE focal surface and observing the OTE beam train in auto-collimating mode, i.e., double-pass configuration, and defines the Sampled-Aperture (SA) test configuration. We assume further that the MWLIs operate continuously and measurements are taken simultaneously. The later requirement is not of importance in this feasibility study since we assume that drifts and vibrations are not present. It is clear that if this study were intended to be more comprehensive, such and other effects would have been taken into consideration.

The two metrology test configurations, i.e., CoC- and SA-test, are depicted in Fig. 2.

- In the CoC-test (see Fig. 2(c)), the measurement beam of the Multi-Wavelength Interferometer (MWLI) goes through the null-lens optics, which is located near the CoC of the PM, and is reflected by the PM back to the MWLI via null lens. The CoC light path is not influenced by the OTE optics other than the PMSEs. The nominal WFE as seen by the CoC-metrology system is depicted in Fig. 3(a).

- In the SA-test (see Fig. 2(a)), the measurement beam of the MWLI is injected at a point on the the OTE focal surface into the OTE optics in reversed order for a particular Field of View (FoV) position. The ACF orientation makes sure that the measurement beam is reflected back via OTE

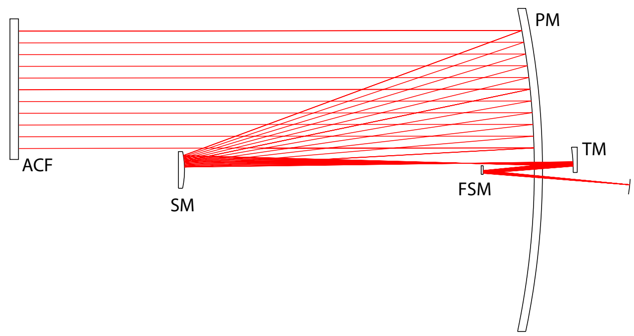

(a) **Sampled-Aperture (SA)** or **Double-Pass Test** in which the SA-test beam is injected at OTE focal surface into the OTE in reversed mode and reflected back via auto-collimating flat (ACF) to its conjugate point.

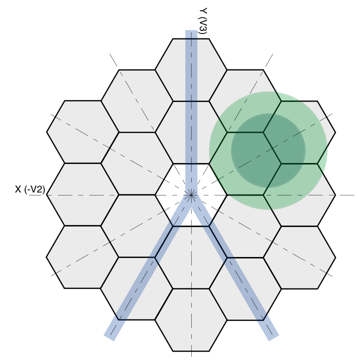

(b) How the ACF will sample the OTE wavefront when using either an ACF having a diameter of either 2400 mm or 1500 mm is depicted.

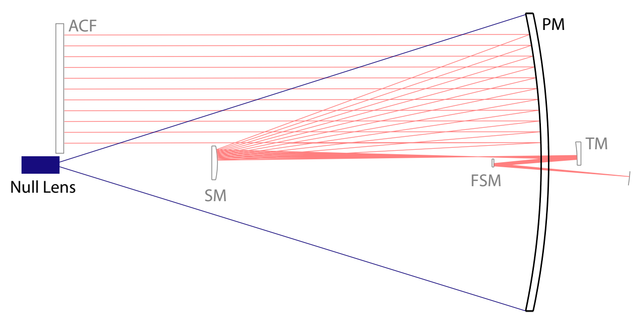

(c) **Centre-of-Curvature (CoC) Test** in which the CoC-test beam measures the figure of the PM with the aid of a null lens placed near the CoC of the PM.

Fig. 2: CoC- and SA-test configurations.

to its conjugate point at the OTE focal surface, which in true auto-collimating mode is the point source position. The SA-test light path is affected by all OTE optical elements as well as by the ACF but remains unaffected by perturbations of the null-lens optics. The nominal WFE as seen by the SA-metrology system is depicted in Fig. 3(b) with an ACF diameter of 2400 mm and in Fig. 3(c) with an ACF diameter of 1500 mm.

When JWST is tested in the quasi-deployed state in the JSC test chamber, the alignment procedure has initially to go through several alignment steps that includes (a) SM focus sweep – finds initial position of SM, (b) PMSE search and identification – determines location on detector of each PMSE, (c) global alignment – better alignment of SM and PMSEs, (d) image stacking – co-aligns the individual PMSE images on top of one another, (e) coarse alignment – decrease wavefront error by adjusting PMSEs piston and (f) fine alignment – final adjustments to the positions of the SM, PMSEs and ACF in order to meet the telescope's Wavefront Error (WFE) performance requirements. In this feasibility study, we assume that the OTE is already well aligned via above mentioned pre-fine-alignment efforts; consequently, only the fine-alignment procedure is of interest.

Table. 1 indicates the optical DoFs for each optical element of primary interest. Some of the DoFs have zero wavefront sensitivities when no figure errors are present; hence, they are not included. Summing them up, we have 141 DoFs (7 DoFs per PMSE (18 PMSEs), 2 DoFs for ACF, 5 DoFs for SM & TM and 3 DoFs for FSM) of which 6 DoFs cannot be controlled.

The initial state errors, i.e., the state of the optical system after completing the coarse alignment, are derived from the JWST error budget, which is determined from the specifications and requirements governing the fabrication and assembly of both the OTE and the test optics as well as the requirements upon the coarse

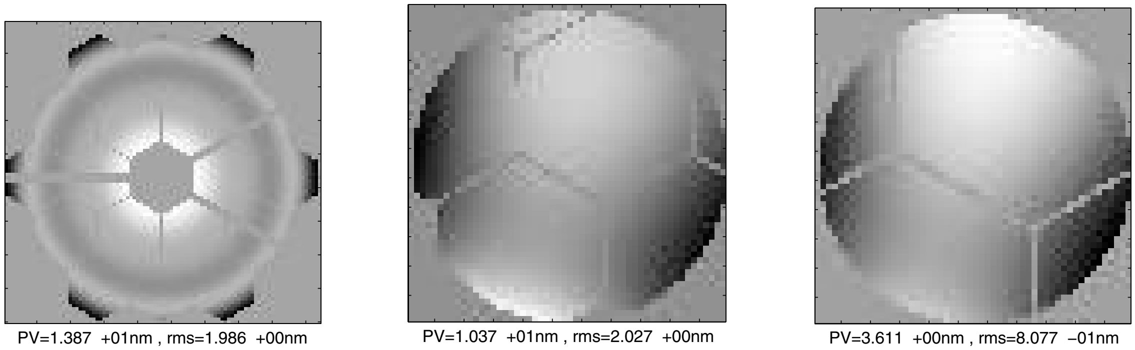

(a) Nominal WFE at CoC sampled with 4866 points

(b) Nominal WFE at SA with ACF=2400mm sampled with 2119 points

(c) Nominal WFE at SA with ACF=1500mm sampled with 2124 points

Fig. 3: Nominal WFE measured at the CoC- and SA-test metrology system. When obtaining the OSE for the DoFs variables, we use approx. 7000 wavefront sampling points (number of rays) leading to a OSE matrix dimension of approx. 7000 by 141 (with 141 active DoFs).

alignment performance. These requirements, which are based upon the anticipated tolerances of the previous mentioned factors, provide error standard deviation values, see Table. 2, for each of the Degree of Freedoms (DoF) of each optical element. For this study, we assume that the initial state errors, control errors and the measurement errors may be expressed as either a process described via Gaussian or Uniform probability statistics, where we assume that they are zero mean based upon incorporation of all known errors into the underlying models. With these presented assumptions, initial state errors of any realisations of the initial optical state of the optical test configuration may now be computed.

Tab. 1: Active Degree of Freedoms (DoFs) are marked by a dark square and "x" identifies those that are also controllable, i.e., they can be actuated. The test optics associated with the CoC-Test, i.e., null-optics, are assumed to be perfect and no figure errors have been included; hence, the twist DoF (Rz) has has for rotationally symmetric elements zero sensitivity.)

	Translation			Rotation			RoC
	Tx	Ty	Tz	Rx	Ry	Rz	
PMSE	X	X	X	X	X	X	X
ACF				X	X		
SM	X	X	X	X	X		
TM	■	■	■	■	■		
FSM			■	X	X		
Null-Optics							

■ Active DoF
X Active Ctrl. DoF

3. ALIGNMENT PROCEDURE

The fine-alignment procedure may be divided up into two groups: a) alignment of the PMSEs to correct for any PM figure errors via the CoC-metrology system and b) alignment of the ACF, SM & FSM via the SA-metrology system.

The Monte Carlo analysis are done as follows: For each realisation, the OTE optics are pertured to tolerances as given in Table. 2 using all observed DoFs. The applied control steps are: a) to align and correct the PM figure back to it's prescription state using all actuators given per PMSE, namely: all six DoFs and RoC correction, b) to align the ACF via tip/tilt correction — it must be noted (see Table. 3) that the actuation errors for the ACF are rather large, c) to align the SM (tip/tilt & decentration DoFs) and FSM (tip/tilt DoFs) and to compensate for residual errors in the OTE.

Tab. 2: Input Statistics for initial element perturbation: entries given for active Degrees of Freedom (limited to this study). (Except for ACF's DoFs, which are Uniform distributed random variables, all other DoFs are Gaussian distributed random variables.)

1-σ std. dev. of Initial Optical State Error Statistics					
	PMSE	ACF	SM	TM	FSM
σ (tip/tilt)	200 urad	$1/\sqrt{3}$ arcmin	200 urad	10 nrad	10 nrad
σ (twist)	286 urad			10 nrad	
σ (decenter)	10 um		20 um	100 nm	
σ (piston)	200 um		20 um	100 nm	100 nm
σ (RoC)	10 nm				

Tab. 3: Input statistics for element actuation: entries given for active Degrees of Freedom (limited to this study). (Except for ACF's DoFs, which are Uniform distributed random variables, all other DoFs are Gaussian distributed random variables.)

1-σ std. dev. Actuation Error Statistics				
	PMSE	ACF	SM	FSM
σ (tip/tilt)	10 nrad	$0.3/\sqrt{3}$ arcsec	1 nrad	10 nrad
σ (twist)	10 nrad			
σ (decenter)	5 nm	$2.5/\sqrt{3}$ mm	2 nm	
σ (piston)	5 nm	$2.5/\sqrt{3}$ mm	2 nm	
σ (RoC)	5 nm			

4. QUICK FEASIBILITY STUDY

The question to be answered here is whether we can align the OTE to the requirements using a single ACF and not significantly increase the risk factors. To quickly address this question, we refrained from using a too complicated system and investigated it with a limited degree of complexity. Normally, we use a non-linear optical system implemented using the MACOS[3,4] optical modelling code but decided that a linearised model is sufficient for this proof-of-concept feasibility study. We used MACOS to linearising the optical system by determining the wavefront sensitivities (WFS) for each observed DoF.[1,5] The resulting WFS matrix can become very large and we limited the sampling of the wavefront observed at the two metrology systems to about 7000 combined data points resulting in a WFS matrix dimension of approx. 7000 by 141 (the number of DoFs used in this feasibility study).

Conducting the fine-alignment study, it was clear that the control of the SM will be non-trivial due to the nature of the test configuration having only a single ACF and therefore sample the SM surface only at a small off-axis area (see Fig. 2(b)). Consequently, the tip/tilt WFS of the SM and the ACF will be very similar and the control will be confused. The confusion will be even more pronounced with increase of wavefront measurement noise.

4.1. OSE versus rms WFE minimisation

During the fine-alignment, we use two different ways of determining the control of the DoFs, which in either case is based upon wavefront measurements. One method of control is to use the OSE where we utilise the estimated state by direct compensation. The other method, refered to as WFE minimisation, is by direct feedback where the wavefront measurements are directly used to determine the feedback control via the gain matrix obtained via Singular-Value Decomposition. The gain matrix is naturally adjusted to different selection of the control DoFs.

As outlined in Sec. 3, the alignment process has a last alignment step where we tweak the adjustments of the SM & FSM to minimise the WFE measured via the SA-test metrology system. Basically, the OSE is used to align the OTE back to its prescription state and then WFE minimisation is applied to optimise the optical performance since the TM cannot be actuated and other error sources limit the capability to obtain this prescription state; hence, we implemented a least square WFE minimisation routine to align both SM & FSM to minimise the WFE in the SA-test metrology system. The results of performing fine-alignment Monte Carlo that go through the entire fine-alignment procedure are depicted in Figs. 4(a)–4(c). The On-Orbit rms WFE performance was not as expected and a quick investigation indicated that the SM is being tilted significantly in the last alignment step. The SA-test configuration with a single static ACF will not sample correctly a SM tilting effect upon the On-Orbit WFE. The SM tilt is to first order sensed as a tilt in the SA-test metrology; consequently, the OSE is being confused with other elements that provide similar wavefront sensitivities. These final alignment step may lead to a superior performance for the SA-test configuration but may also lead to an inferior performance for the On-Orbit (OO) configuration (without test optics).

What performance can be expected if we just leave the OTE in the alignment state as obtained via OSE only, i.e., we will not minimise the WFE in the SA-test metrology system. The results of this are depicted in Figs. 4(d)–4(f), which indicate that in spite of the overall slightly inferior performance in the SA-test, the On-Orbit rms WFE is significantly reduced, i.e., better alignment of the OTE.

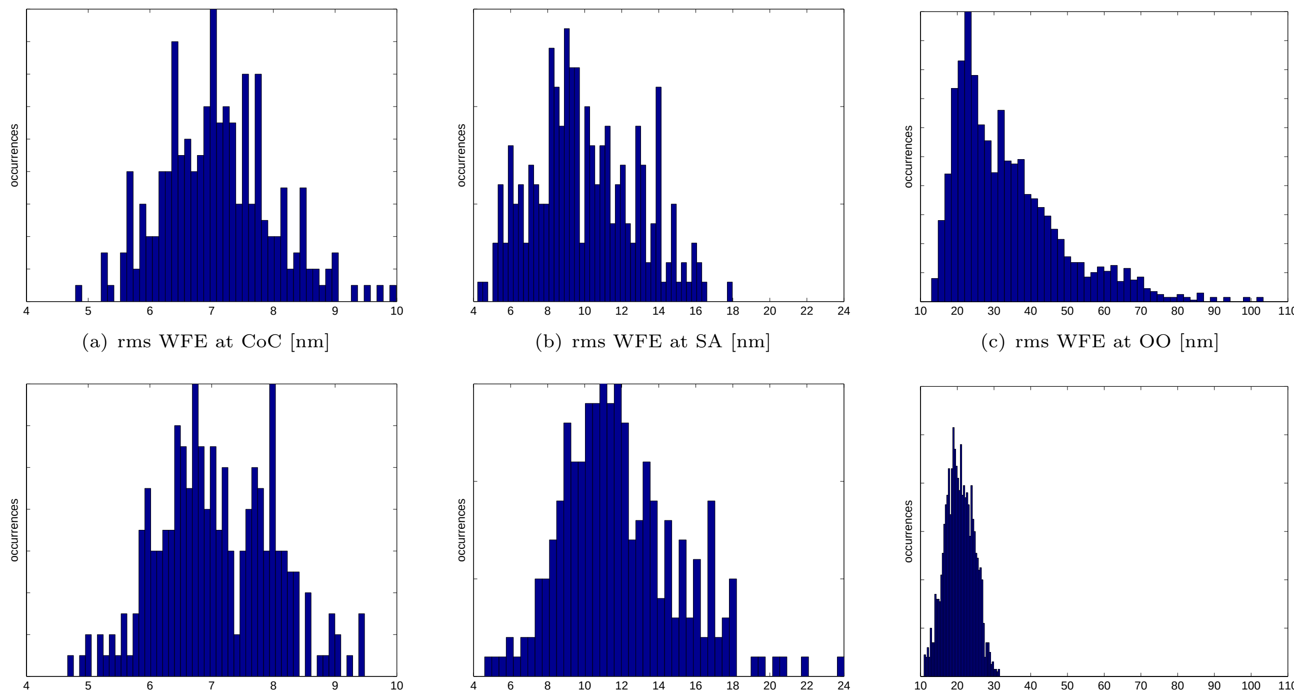

(a) rms WFE at CoC [nm]
(b) rms WFE at SA [nm]
(c) rms WFE at OO [nm]
(d) (OSE) rms WFE at CoC [nm]
(e) (OSE) rms WFE at SA [nm]
(f) (OSE) rms WFE at OO [nm]

Fig. 4: WFE histograms at the two test setups (CoC & SA) and with the test optics removed, i.e., On-Orbit (OO) config. Figs. 4(a)–4(c) show cases when WFE minimisation is applied while Figs. 4(d)–4(f) show cases when only the OSE is used for alignment. These results are based upon an ACF mirror diameter of 2400 mm, 250 Monte-Carlo realisations and an one-sigma std. dev. wavefront measurement error (WFME) of σ=3nm. For easy comparison, corresponding plots are plotted over the same WFE range (x-axis).

4.2. ACF Size Influence

A significant question is also whether the amount of information loss due to reducing the sampling area of the OTE wavefront will be significant enough not to be able to align the OTE. An ACF having a diameter of 2400 mm is more expensive to manufacture, to mount and to actuate than one having a diameter of 1500 mm.

An illustration of how the two ACFs sample the OTE is given in Fig. 2(b). For simplicity and the quickness, the smaller ACF was not relocated in order to find its most effective position.

As outlined in the previous section, we go through the complete fine-alignment procedure for every of the 250 Monte Carlo runs where we either apply the rms WFE minimisation or not. The results of these analyses are depicted in Fig. 5, which clearly show that in spite of the overall slightly inferior performance in the SA-test Fig. 5(b) configuration, the On-Orbit rms WFE is significantly lower when using the OSE and not applying the rms WFE minimisation control. In spite of the reduced sampling area, it was feasible to align the OTE and to obtain relative small rms WFE in the on-orbit configuration. The other conclusion that one may draw is that larger is better and since we have a very benign overall perturbation of the optical system, i.e., no figure errors on any of the optical elements, no process noise and not using full DoF of entire system, it is predictable that the fine-alignment will become very difficult in the presence of other error sources, which will be demonstrated in Sec. 4.3.

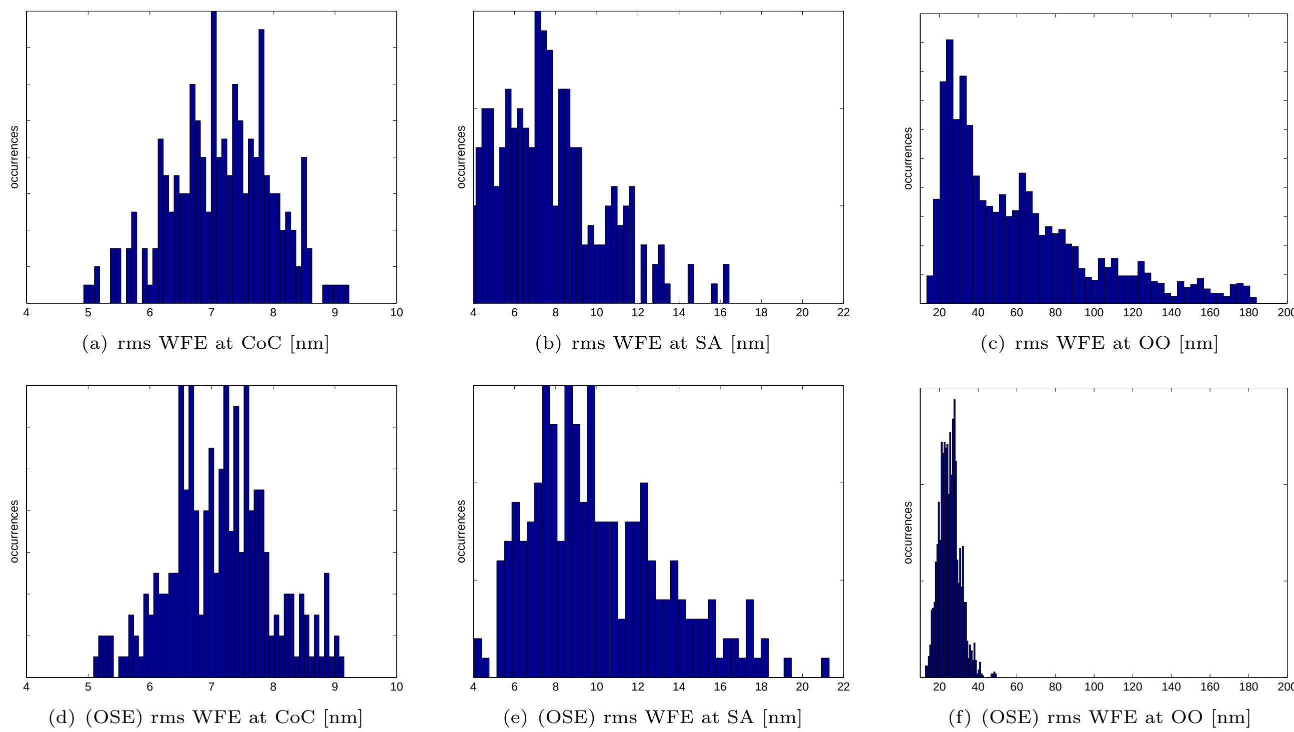

(a) rms WFE at CoC [nm] (b) rms WFE at SA [nm] (c) rms WFE at OO [nm]

(d) (OSE) rms WFE at CoC [nm] (e) (OSE) rms WFE at SA [nm] (f) (OSE) rms WFE at OO [nm]

Fig. 5: WFE histograms at the two test setups (CoC & SA) and with the test optics removed, i.e., On-Orbit config. Figs. 5(a)–5(c) show cases when WFE minimisation is applied while Figs. 5(d)–5(f) show cases when only the OSE is used for alignment. These results are based upon an ACF mirror diameter of 1500 mm, 250 Monte-Carlo realisations and an one-sigma std. dev. wavefront measurement error (WFME) of σ=3nm. For easy comparison, corresponding plots are plotted over the same WFE range (x-axis).

4.3. Wavefront Measurement Error Influence

A commercially available multi-wavelength interferometer (MWLI) is currently capable of providing high resolution interferometric measurements that are insensitive to vibration and have a synthetic wavelength coverage from 18um up to 10mm (in discrete steps) besides the two fundamental wavelengths. The amount of measurement uncertainty is linked to the synthetic wavelength. This means that as we align the optical system and reducing therefore the WFE, the measurement uncertainty is decreasing as we use shorter synthetic wavelengths. The expected amount of measurement uncertainty in the final alignment state may vary; consequently, we will conduct a quick investigation of the dependence of the fine-alignment performance as function of wavefront measurement uncertainty. To simplify the modelling, we will not include the full MWLI model and just assume that the wavefront measurement uncertainty is constant during the fine-alignment process.

The results of this investigation are presented in Figs. 6–7, which are based upon an ACF diameter of 2400 mm, and Figs. 8–9, which are based upon an ACF diameter of 1500 mm. As expected, the resulting WFE using the smaller ACF is larger than with the larger ACF. Independent of the ACF size, the benefit of only using the OSE to align the system has been demonstrated; however, with increase of WFME, the OSE becomes confused between the DoFs as it cannot differentiate between the wavefront sensitivities (WFS) characterizing each DoF. Hence, the effectiveness of the OSE reduces with increase of WFME with the current design of the OSE.

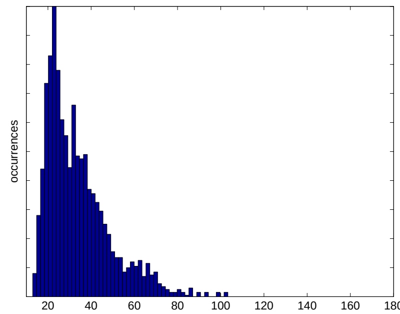

(a) σ=3nm, rms WFE at OO [nm]

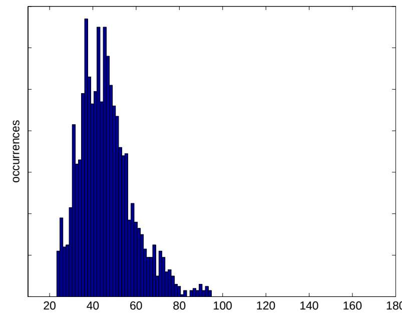

(b) σ=6nm, rms WFE at OO [nm]

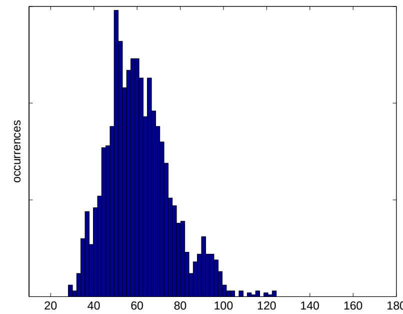

(c) σ=9nm, rms WFE at OO [nm]

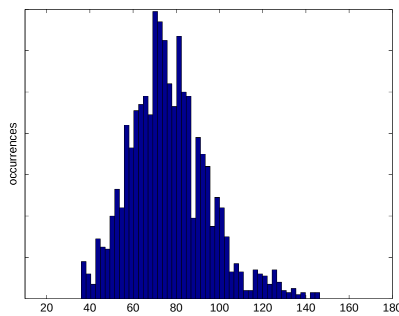

(d) σ=12nm, rms WFE at OO [nm]

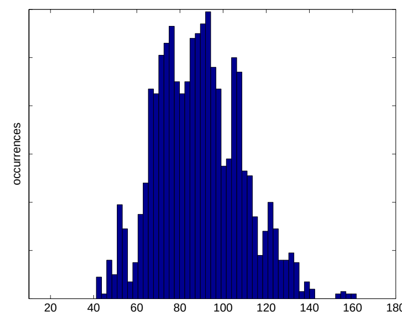

(e) σ=15nm, rms WFE at OO [nm]

Fig. 6: On-Orbit rms WFE results that are based upon 250 Monte Carlo realisations with an ACF diameter of 2400 mm.

5. CONCLUSION

Our quick investigation indicates that a significant amount of effort must be invested in order to align the OTE using a single static ACF with confidence when all other factors and uncertainties will come into play as well.

Options like rotating the ACF and therefore ensuring that the footprint on the SM is significantly altered might be an alternative in order to mitigate alignment errors due to control confusions. Adding more field points, to which the ACF needs to be oriented, over the instrument FoV ($\approx \pm 10$ arcmin) will not add enough information — in spite of introducing field-dependent aberration information — to mitigate control confusion since the associated footprints on the SM will not significantly shift and therefore not adequately sample the SM.

It must be emphasised that in this feasibility study, we simplified the modelling of the ground test at JSC; hence, any increase in complexity demands for more information obtained from the wavefront measurements (and maybe also from other means). For instance, we have ignored effects of vibration and drifts, figure errors on all optical elements (prescription errors and gravity sag influence, which have a known and unknown component), calibration errors in the CoC-test, that the source position and direction of the SA-metrology beam is erroneous, that a global alignment of the PM must be conducted to align the CoC- and SA-test axes (PM and CoC-optics must move together), that we do not model the entire MWLI alignment process and all unknown unknowns.

This preliminary study gives indication that a single ACF with a single field point is probably not providing enough information to align the system to the JWST requirements; consequently, we will investigate the feasibility to align the OTE using a three-mirror ACF configuration, which will probably significantly reduce the risks.

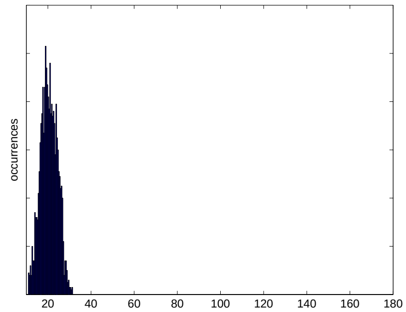

(a) (OSE) σ=3nm, rms WFE at OO [nm]

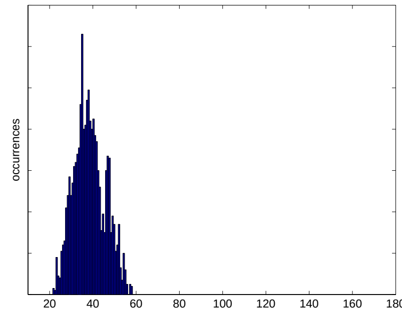

(b) (OSE) σ=6nm, rms WFE at OO [nm]

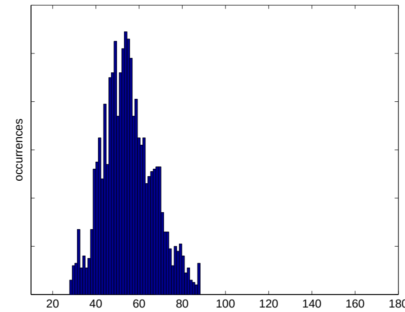

(c) (OSE) σ=9nm, rms WFE at OO [nm]

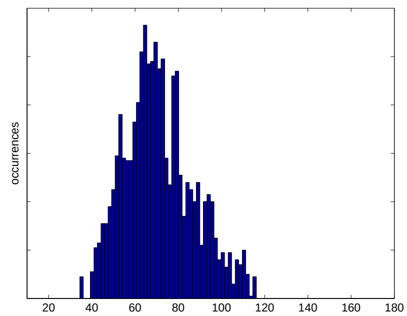

(d) (OSE) σ=12nm, rms WFE at OO [nm]

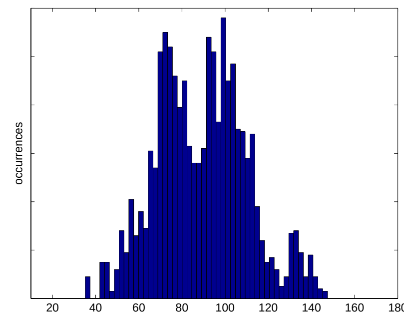

(e) (OSE) σ=15nm, rms WFE at OO [nm]

Fig. 7: On-Orbit rms WFE results that are based upon 250 Monte Carlo realisations with an ACF diameter of 2400 mm and using OSE based control only.

6. ACKNOWLEDGMENTS

This work was performed at the Jet Propulsion Laboratory, California Institute of Technology, under contract with the National Aeronautics and Space Administration.

REFERENCES

1. D. C. Redding, N. Sigrist, J. Z. Lou, Y. Zhang, P. D. Atcheson, D. S. Acton, and W. L. Hayden, "Optical state estimation using wavefront data," *Current Developments in Lens Design and Optical Engineering V* **5523**(1), pp. 212–224, SPIE, 2004.
2. James Webb Space Telescope's web-site: http://www.jwst.nasa.gov/.
3. D. C. Redding, *Modeling and Analysis for Controlled Optical Systems (MACOS)*. Jet Propulsion Laboratory.
4. D. C. Redding and W. Breckenridge, "Optical modeling for dynamics and control analysis," *Journal of Guidance, Control, and Dynamics* **14**, Sept.-Oct. 1991.
5. J. M. Howard, "Optical modeling activities for the James Webb Space Telescope (JWST) project: I. The linear optical model," *Optical Modeling and Performance Predictions* **5178**(1), pp. 82–88, SPIE, 2004.

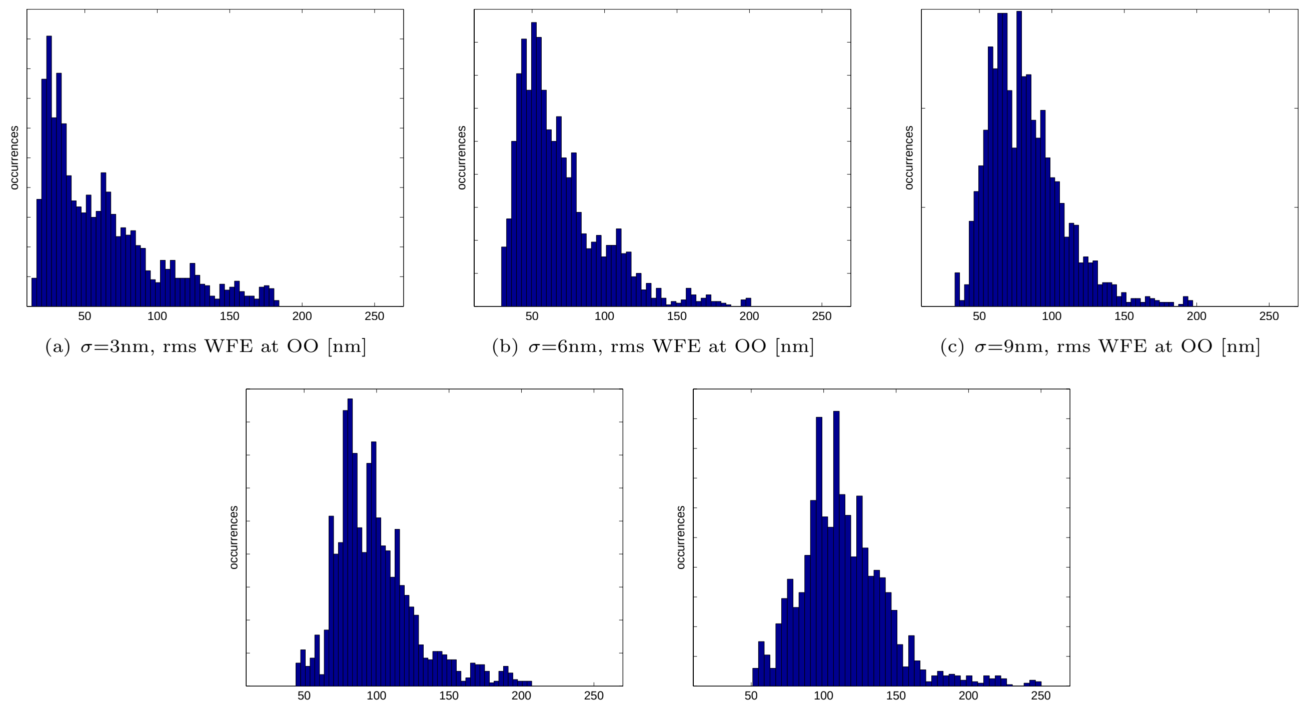

(a) σ=3nm, rms WFE at OO [nm] (b) σ=6nm, rms WFE at OO [nm] (c) σ=9nm, rms WFE at OO [nm]

(d) σ=12nm, rms WFE at OO [nm] (e) σ=15nm, rms WFE at OO [nm]

Fig. 8: On-Orbit rms WFE results that are based upon 250 Monte Carlo realisations with an ACF diameter of 1500 mm.

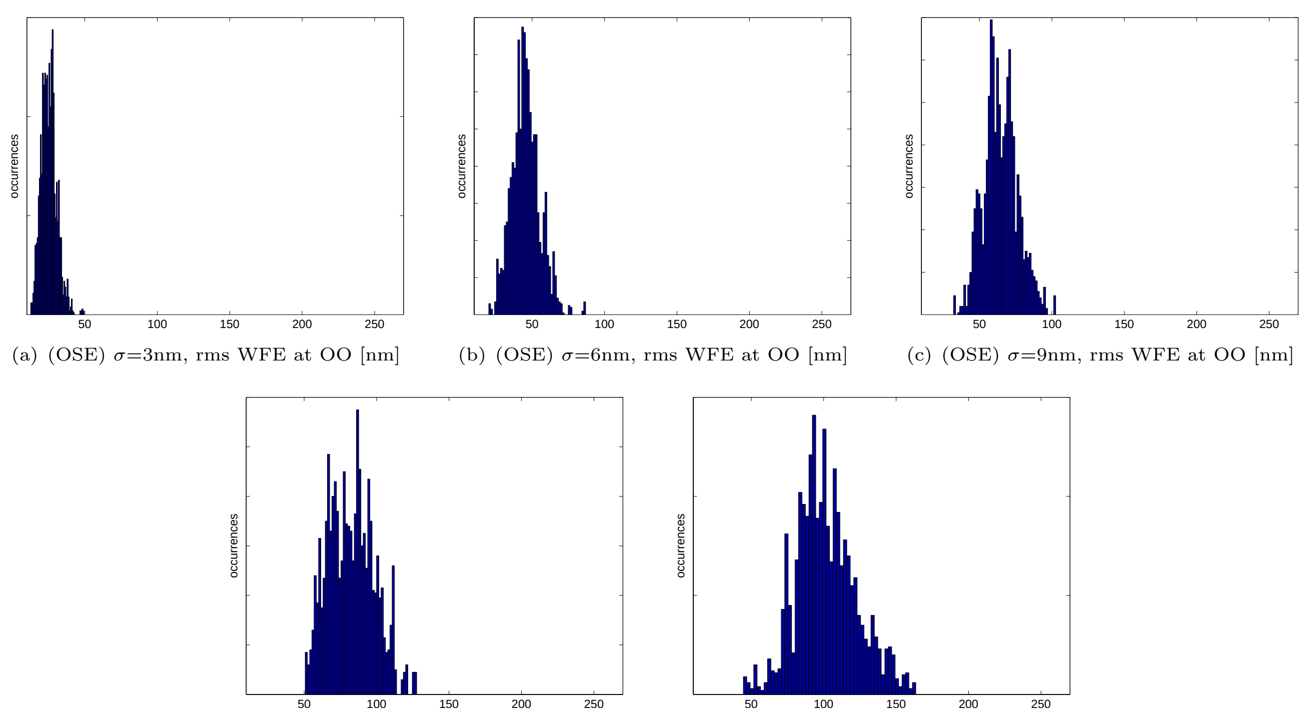

(a) (OSE) σ=3nm, rms WFE at OO [nm] (b) (OSE) σ=6nm, rms WFE at OO [nm] (c) (OSE) σ=9nm, rms WFE at OO [nm]

(d) (OSE) σ=12nm, rms WFE at OO [nm] (e) (OSE) σ=15nm, rms WFE at OO [nm]

Fig. 9: On-Orbit rms WFE results that are based upon 250 Monte Carlo realisations with an ACF diameter of 1500 mm and using OSE based control only.